Nigel P. Beard
Joshua B. Edel
Andrew J. deMello

Department of Chemistry,
Imperial College London,
Exhibition Road,
South Kensington,
London, UK

Integrated on-chip derivatization and electrophoresis for the rapid analysis of biogenic amines

We demonstrate the monolithic integration of a chemical reactor with a capillary electrophoresis device for the rapid and sensitive analysis of biogenic amines. Fluorescein isothiocyanate (FITC) is widely employed for the analysis of amino-group containing analytes. However, the slow reaction kinetics hinders the use of this dye for on-chip labeling applications. Other alternatives are available such as *o*-phthaldehyde (OPA), however, the inferior photophysical properties and the UV λ_{max} present difficulties when using common excitation sources leading to a disparity in sensitivity. Consequently, we present for the first time the use of dichlorotriazine fluorescein (DTAF) as a superior *in situ* derivatizing agent for biogenic amines in microfluidic devices. The developed microdevice employs both hydrodynamic and electroosmotic flow, facilitating the creation of a polymeric microchip to perform both precolumn derivatization and electrophoretic analysis. The favorable photophysical properties of the DTAF and its fast reaction kinetics provide detection limits down to 1 nM and total analysis times (including on-chip mixing and reaction) of $<$60 s. The detection limits are two orders of magnitude lower than current limits obtained with both FITC and OPA. The optimized microdevice is also employed to probe biogenic amines in real samples.

Keywords: Biogenic amines / Dichlorotriazine fluorescein / Microchip electrophoresis / Miniaturization
DOI 10.1002/elps.200305919

1 Introduction

Amines that participate in biological activities and that exist widely in nature are often collectively known as biogenic amines. It is recognized that many biogenic amines are essential to living systems [1]. However, at certain levels they have been deemed to promote adverse effects on human health. For example, a variety of malignant cell propagations have been allied with the presence of increased biogenic amine levels. It has been suggested that certain concentrations of polybiogenic amines in urine can be manipulated as indicators of cancerous tumors [2]. Biogenic amines can also be found in a variety of foods and beverages. In particular, fermented products such as cheese [3, 4], red wine [5, 6] and soy sauce [7, 8], and protein-rich foods such as fish [9] and meat [10]. Ingestion of high amounts of biogenic amines can result in symptoms of intoxication such as nausea, migraines or asthma [11, 12]. The study of biogenic amines is not only of interest for their toxicological risk, but also as an indicator of food quality.

A variety of methods have been employed to determine biogenic amines both qualitatively and quantitatively. Given that biogenic amines exhibit no natural UV absorption or fluorescence, they have traditionally been determined either by analyte derivatization or in their native form by indirect detection. The majority of these methods include extraction and subsequent analysis by high-performance liquid chromatography (HPLC) [13–16]. However, the analysis of biogenic amines by capillary electrophoretic techniques have also been reported [17–19]. For example, Arce and co-workers [20] demonstrated the electromigrated separation of 21 amino compounds by capillary zone electrophoresis (CZE) with indirect UV absorption. In addition, the separation of biogenic amines has been performed by chip-based MEKC (micellar electrokinetic chromatography) with analyte derivatization using FITC [21]. The separation of eight biogenic amines by microchannel MEKC was facilitated by employing an anionic surfactant, with detection limits in the region of 3–6 μM In a previous paper [22], we developed a microdevice for the analysis of biogenic amines in their natural

Correspondence: Dr. Andrew J. deMello, Department of Chemistry, Imperial College London, Exhibition Road, South Kensington, London, SW7 2AY, UK
E-mail: a.demello@ic.ac.uk
Fax: +44-(0)-207-594-5834

Abbreviations: DTAF, dichlorotriazine fluorescein; **his**, histamine; **OPA**, *o*-phthalaldehyde; **PDMS**, polydimethylsiloxane; **put**, putrescine; **TCSPC**, time-correlated single photon counting system; **trp**, tryptamine

form by employing indirect fluorescence detection (IFD) and achieved limits of detection comparable with those reported by the FITC-labeling technique. However, we noted that due to the fact that IFD methods are inherently not selective to the functional group of the target analyte but the overall charge, an integrated *in situ* fluorescent tagging method would be preferential in both maintaining the speed of analysis and solving the difficulties associated with IFD. This would not only improve on the selectivity of the method but also improve the sensitivity. There are two approaches to performing integrated labeling on chip: post- and pre-column derivatization [23–27]. Recently, Ro *et al.* [28] have performed pre-column on-chip labeling of biogenic amines using the derivatizing agent *o*-phthaladehyde (OPA) followed by separation by MEKC. Surprisingly, detection limits of only 0.1 μM are quoted using laser-induced fluorescence (LIF) detection. It is noted that even though the limit of detection reported is adequate for certain foods, samples containing smaller levels would prove difficult to analyze. This disparity in sensitivity is mainly due to the inferior photophysical properties of the OPA dye when compared to its visible counterpart FITC. FITC has proved to be a popular fluorescent derivatizing agent for the amino functionality, primarily due to its high quantum yield (~0.92), and its λ_{max} (492 nm) matching that of the output of the commercial argon-ion laser (λ_{max} = 488 nm). However, the extremely slow kinetics associated with the derivatization reaction (often ~12 h) completely negate the inherent benefits of microchip CE. These include improved efficiencies with respect to sample size, sample throughput and especially with respect to the speed of analysis. The speeds at which separations can be realized in the microchip domain have out-performed their conventional counterparts significantly. Consequently, derivatization chemistries that function on similar timescales are desirable if pre-column derivatization and electrophoretic analysis are to be effectively integrated within monolithic chip systems.

In this paper we demonstrate the use of an alternative fluorescent label for the analysis of biogenic amines, namely dichlorotriazine fluorescein (DTAF). Due to its good stability, rapid derivatization kinetics and excellent photophysical characteristics DTAF allows for the efficient integration of pre-column derivatization and electrophoretic analysis on a monolithic device.

2 Materials and methods

2.1 Microchip fabrication

The layout of the CE microchip used in this work is shown schematically in Fig. 1. Unless stated otherwise, the detection window is positioned 30 mm from the

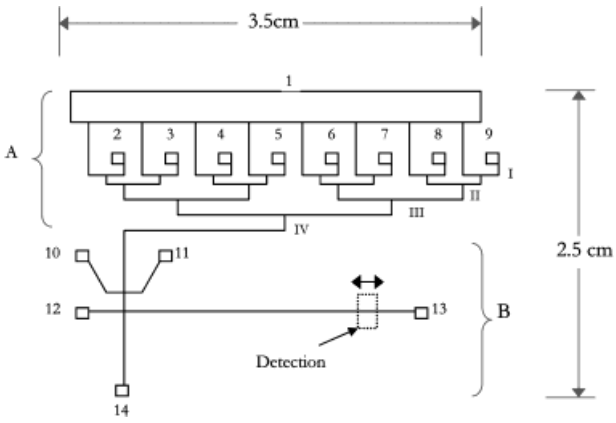

Figure 1. Schematic diagram of microchip layout. (1) common reaction buffer reservoir; (2)–(9) sample reservoirs; (10), (11) additional sample focusing/control reservoir; (12), (13) separation buffer reservoirs; (14) flow control reservoir (under negative pressure). I, II, III and IV are respective mixing junctions throughout the fluidic network. Area A defines the mixing zone, and area B defines the electrophoretic separation zone.

injection for all analyses. The final device comprised an unstructured glass substrate and a polydimethylsiloxane (PDMS) moulded layer containing the microchannel network. Fabrication of the PDMS layer involved a three-step process: (i) the fabrication of a chromium mask, (ii) the generation of an SU-8 master, (iii) the moulding of the device in PDMS. Brief details of each step are now presented. First, the channel pattern was created using AutoCAD 95© and transferred onto a glass wafer pre-coated with a positive photoresist layer and a chromium layer (Nanofilm; Westlake Village, CA, USA) using a direct-write photolithographic system (DWL2.0; Heidelberg Instruments, Heidelberg, Germany). The exposed photoresist was first removed using a mixture of developing agent (Microposit, Coventry, UK) and water (5:1). This was followed by chromium removal using a Lyodyne etch solution (Microchem Systems, Coventry, UK). This resulted in a transparent microchannel layout of the chip design. Next, a plain glass wafer was spin-coated with a negative photoresist XP SU-8 10 (Microchem, Newton, MA, USA) at 2500 rpm yielding a 12 μm (± 1 μm) thick resist layer. The transparent channel network on the chromium mask was then transferred onto the SU-8 substrate by contacting the substrates and exposing under a 10 cm diameter collimated UV beam from a 200 W mercury lamp (Goulding and Partners, Sussex, UK). The unexposed SU-8 was then removed using 1,2-propanediol monomethyl ether acetate (PMEA) (Lancaster, Morecambe, UK), leaving the SU-8 network fixed to the glass substrate. This was then baked for 24 h at 120°C. To form the structured PDMS layer, PDMS base and curing agent

(Sylgard 184; Dow Corning, Wiesbaden, Germany) were mixed in a ratio of 10:1 w/w, degassed and decanted onto the SU-8 master. The resulting structure was cured overnight in an oven at 40°C. One common buffer reservoir (approximately 6 cm × 2 cm) was cut at the top of the micro device providing a central reservoir for the label and reaction buffer. Sample reservoirs were created by punching square holes of side 500 μm at the end of the sample channels of each CE system using a specially constructed bradawl. The PDMS substrate and a plain glass wafer were cleaned with 1 M sodium hydroxide and ethanol before being brought into contact to form the complete microfluidic chip.

2.2 Optical detection system

An inverted microscope (DMIL; Leica, Milton Keynes, UK) equipped with a filter cube comprising an excitation filter (band pass 450–490 nm), a dichroic mirror, a reflection short pass filter (510 nm), and a suppression filter (band pass 515–560 nm) was used for detection. Excitation light (488 nm, 10 mW) from air-cooled argon-ion laser (Melles-Griot, Cambridge, UK) was passed through the excitation filter, reflected by the dichroic mirror and focused onto the microchip. Fluorescence emission was collected by a microscope objective (10×, 0.42 NA) (Newport, Irvine, CA, USA), passed through the dichroic mirror, a suppression filter, and finally through an adjustable detection window set at 20 μm × 40 μm. A photomultiplier tube (MEA153; Seefelder Messtechnik, Germany) functioning in current mode was employed to detect fluorescence photons. Data were acquired at a frequency of 20 Hz, stored using a PC data acquisition program (Picolog; Pico Technology, Hardwick, Cambridge, UK) and processed in Origin 6.0 (Microcal Software, Northampton, USA). An in-house 8-channel power supply was used to supply the drive voltages for electrophoresis and operated between 0 and +3000 V relative to ground. Voltage control was affected using a programme written under the LabView 5.0 graphical programming environment (National Instruments, Austin, TX, USA).

2.3 Time-correlated single photon counting system

A time-correlated single photon counting system (TCSPC) system was employed for fluorescence lifetime measurements. The setup consisted of a 438 nm picosecond pulsed diode laser (PicoQuant) excitation source driven by a PDL 800-B driver (PicoQuant). The driver unit contains a built in pulse generator which produces a master frequency of 40 MHz that can be divided by factors of 1, 2, 4, 8, 16 to produce selectable frequencies of 40, 20, 10, 5, 2.5 MHz. An external function generator (TTi, electronics, UK) was coupled to the external trigger input of the driver so that lasing repetition frequencies could be controlled and varied between 100 kHz and 40 MHz. Fluorescence was collected perpendicular to the excitation source using a silicon avalanche photodiode detector (SPCM-AQR-131; EG&G Canada, Vaudreuil, Quebec, Canada). The electronic output from the detector was coupled to a multichannel scalar (MCS-PCI; EG&G), and to a TimeHarp 200 (PicoQuant) TCSPC card for fluorescence lifetime measurements.

2.4 Reagents, buffers, and sample solutions

The biogenic amine standards putrescine (Put), histamine (His) and tryptamine (Try) were 97–99% pure, (Sigma-Aldrich, Gillingham, Dorset, UK). Running buffer solutions were made from sodium borate (Sigma-Aldrich) and 0.1 M sodium hydroxide solution. The Thai Fish Sauce (Blue Dragon, Kent, UK) was used as received. To improve amine solubilization in the separation medium, a small percentage of 2-propanol (~3% v/v) was added to the running buffer. This procedure has been well documented as an efficient way of encouraging hydrophobic compounds to stay in an aqueous environment [29]. All experiments were carried out using freshly prepared and filtered solutions.

2.5 Microchip design and rational

The layout of the microdevice designed for this work is shown schematically in Fig. 1. The device can be categorized by two distinct zones a 'derivatisation' zone (A) and a 'separation' zone (B). The derivatisation zone comprises fifteen parallel 'T'-junctions that unite through a symmetrical network of microfabricated channels. Each of the eight terminal 'T'-junctions is serviced by a common reaction buffer reservoir and a sample reservoir. The derivatization zone (A) allows for diffusive mixing and reaction of the reagents, and is controlled by applying negative pressure to reservoir (14). Negative pressure was used to motivate fluid in the derivatization zone, since this method also provided a natural vacuum between the PDMS microstructure and the soda lime glass base plate, thus ensuring no lifting of the PDMS layer from the glass substrate. More importantly, negative pressure provides simple operation requiring only a single reservoir to be under pressure to control the whole mixing zone. Employing hydrodynamic forces to facilitate diffusive mixing brings with it several major advantages over controlling the entire device by elec-

troosmotic flow (EOF). Firstly the number of electrodes/power sources to control the device is kept to a minimum providing simplicity in operation. Secondly, sample biasing (usually associated with electrokinetic injection) is eliminated. Furthermore, when using EOF the double layer present at the channel wall and solution interface needs to be extremely reproducible to facilitate accurate and equal flow of all fluids through the derivatizing zone. This requirement is not necessary when employing hydrodynamic fluid manipulation. The device is therefore enhanced by the benefits of both hydrodynamic forces during the mixing and reaction zone, and electroosmotic forces to facilitate separation. The combination of differing forces within the same microdevice has seen increasingly popularity in recent years [30–33]. For example, Chien and co-workers [34–37] have published various papers where fluid manipulation of samples/reagents is facilitated by hydrodynamic flow control followed by electrophoretic separation.

The second area of the microfluidic device is dedicated to the electrophoretic separation of the products. Reservoirs (12) and (13) serve as the buffer inlet and buffer outlet of the separation channel, providing a maximum effective separation length of 35 mm. However, due to the hydrodynamic forces used throughout the derivatization zone, it was found that further control of the sample stream during the separation was necessary. Subsequently, an additional set of pinching channels was introduced into the layout to facilitate the degree of control required. This design change brought two distinct benefits to the finished microdevice. Firstly it allowed the control of the sample stream after injection, preventing sample leakage into the separation channel during the separation phase. Secondly, a more optimal injection plug shape and width is achieved. In traditional injectors the formed sample plug is subject to broadening in the *x*-direction resulting in a 'trapezoidal' shaped plug. The additional channels provide a much narrower and symmetrical sample plug at the separation channel intersection curtailing band broadening and improving separation efficiency. Optimization of sample plug profiles by this method was initially identified by Bousse and coworkers [38, 39].

2.6 Microchip operation

The empty microdevice was first filled with ethanol by capillary action. This process was crucial to ensure efficient operation, and permitted subsequent aqueous solutions to be introduced directly into the somewhat hydrophobic PDMS channels. The electroosmotic flow observed in the PDMS channels was similar in magnitude to that seen in equivalent glass-etched channels. Consequently, no surface modification of the PDMS channels was performed before operation. Electrical contact between the high voltage power supply and fluidic reservoirs (10, 11, 12, and 13) was made using platinum electrodes. The device was then operated in two steps 'mixing/reaction' and 'separation' mode. During the 'mixing/reaction' mode, sample from each of the sample reservoirs (2–9) was drawn under negative pressure with the label and reaction buffer from the common reservoir (1). Each stream of sample is brought into contact with the reaction buffer at intersection (I) of the mixing zone. Mixing is entirely dependent on mass transport by diffusion, and proceeds throughout the derivatization zone into one mixed and reacted sample stream. The resultant sample stream is drawn across the separation channel and forms the sample plug at the intersection. The total time to achieve plug formation is approximately 20 s. Once the sample plug has been formed the next stage is injection and separation. Subsequently a voltage of $\leq +3.0$ kV is applied to the inlet buffer reservoir (12) whilst the outlet buffer reservoir (13) is grounded. This operation moves the sample plug formed at the cross-intersection into the separation channel and electrophoresis proceeds. To prevent leakage from the sample channel into the separation channel during this operation, an optimized control voltage of $+1.0$ kV is applied to reservoirs 10 and 11 for the duration of the separation.

3 Results and discussion

3.1 Optimization of derivatization zone

When addressing the nature of mixing in microfluidic networks, an understanding of the behaviour of fluids is requisite. As an approximate rule, the Reynolds number (R_e) of a fluid through a device can be employed to express the type of flow possible, and holds the following relationship:

$$R_e = \frac{D_{eq} \nu_{av} \rho}{\mu} \quad (1)$$

where D_{eq} is the cross-sectional area of the channel through which the fluid flows, ν_{av} is the average velocity of the fluid, ρ is its density, and μ is its viscosity. Under most circumstances a $R_e > 2000$ results in turbulent flow and a $R_e \ll 2000$ affords laminar flow. In our microchip flow rates are typically $\ll 1$ mL/min, thus D_{eq} becomes the dominating factor, and low R_e values result. Therefore flow is laminar and mixing occurs by diffusion based mass-transport mechanism only. Consequently,

the microchip derivatization zone needs to provide a route to maximize this mechanism in the shortest possible time. Designs can be qualified using Ficks Law:

$$t = \frac{(\Delta x)^2}{2D} \quad (2)$$

where $(\Delta x)^2$ is the diffusion distance in the *x*-direction (cm^2) and *D* is the diffusion coefficient of the molecule (cm^2s^{-1}). It is therefore beneficial to create a device that minimizes the term $(\Delta x)^2$, and this formed the first part of the optimization of the microdevice. The chip design outlined in Fig. 1, illustrates a mixing zone incorporating several small and evenly distributed fluid streams which combine over a short distance. This minimizes the diffusion distance and the striation thickness. Other designs were studied; however, this proved to be the most efficient. Further optimization of the mixing zone was investigated by reducing the channel width (*x*) of the mixing zone. Effects of such variations were assessed by visualization of a homogeneous fluorescence quenching reaction. The efficiency of each different mixing zone was determined by observing the quenching of fluorescein (500 μM) by hydrochloric acid (0.1 M). As this reaction proceeds *via* rapid proton transfer, the degree of quenching is effectively determined by diffusional mixing. The effect of decreasing the channel width $(\Delta x)^2$ is illustrated in Fig. 2. For each of the different mixers, measurements were recorded at the respective junctions (I, II, III, and IV). The results in Fig. 2 qualitatively agree with Eq. (2), in that the narrowest channels provide the fastest route to complete

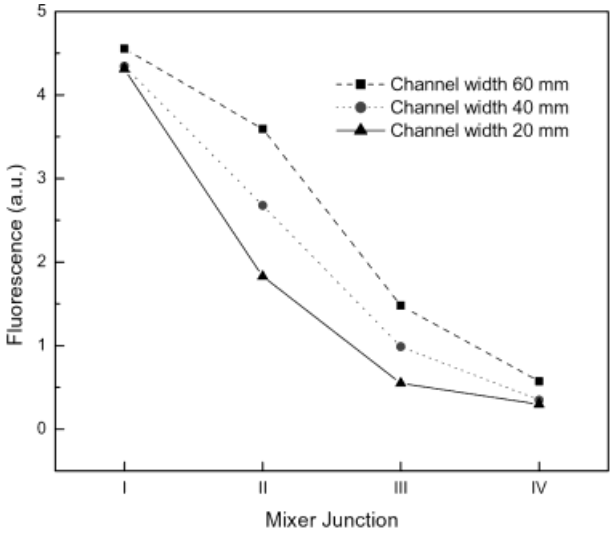

Figure 2. Variation of mixing efficiency with channel width (*x*). Quenching reaction between 500 μM fluorescein in 80 mM borate buffer at pH 8, with 0.1 M hydrochloric acid. Each fluorescent data point recorded at the respective junction within the mixing zone (I, II, III and IV) employing a detection window of 40 μm × 40 μm.

diffusion. It is worth noting that channel widths below 20 μm were investigated, however channel blockages and non-uniform pressure distribution throughout the mixing zone became apparent. Therefore the optimum channel width providing reproducible and efficient mixing was found to be 20 μm and subsequently employed in all further experiments. Channels were 12 μm deep.

3.2 Suitability of DTAF as a labeling moiety for biogenic amines

As stated previously, the most common fluorescent derivatizing agent for the amino functionality is the fluorophore FITC (λ_{max} = 492 nm). This is not only due to its high quantum yield (0.92), but also, the photophysical properties of the dye are ideally suited to excitation by argon-ion lasers (488 nm). However, the primary drawback when using FITC is the extremely slow reaction kinetics. It has been reported that in the case of biogenic amines, reaction times can be up to 12 h [8]. This attribute alone makes FITC unsuitable for use in rapid *in situ* labeling methods. Consequently, an investigation into suitable amino group probes was required to facilitate a successful derivatizing agent. An amine reactive dichlorotriazine probe containing the fluorophore fluorescein (DTAF) has been established as a suitable label for amines [40]. However, DTAF has seen very little use and is frequently cast aside for the more popular FITC molecule. One possible reason for this is that DTAF and the conjugates it forms are relatively unstable in water if left for long periods of time [41], a disadvantage of no consequence in the fast and efficient environment of the microchip. The derivatization route for DTAF and the biogenic amines studied is outlined in Fig. 3. The photophysical properties of DTAF are also excellent. Table 1 illustrates some of the photophysical properties of DTAF and FITC for comparison. It is evident from these data that DTAF is equivalent to FITC in all areas, and even superior in the case of quantum yield. It is also important to note that the extinction coefficient of FITC has been reported to decrease approximately 10% upon conjugation [42].

Table 1. Fluorophore characteristics of DTAF and FITC

Fluorophore	Molecular weight	λ_{max} (nm)	Extinction coefficient[a)] (ε)	Quantum yield [c)] (Φ_f)	λ_{em} (nm)
DTAF	495.28	492	84,000	0.92	516
FITC	389.38	494	76,000	0.92	519

a) Data were obtained from Jackson Immunoresearch, PA, USA.

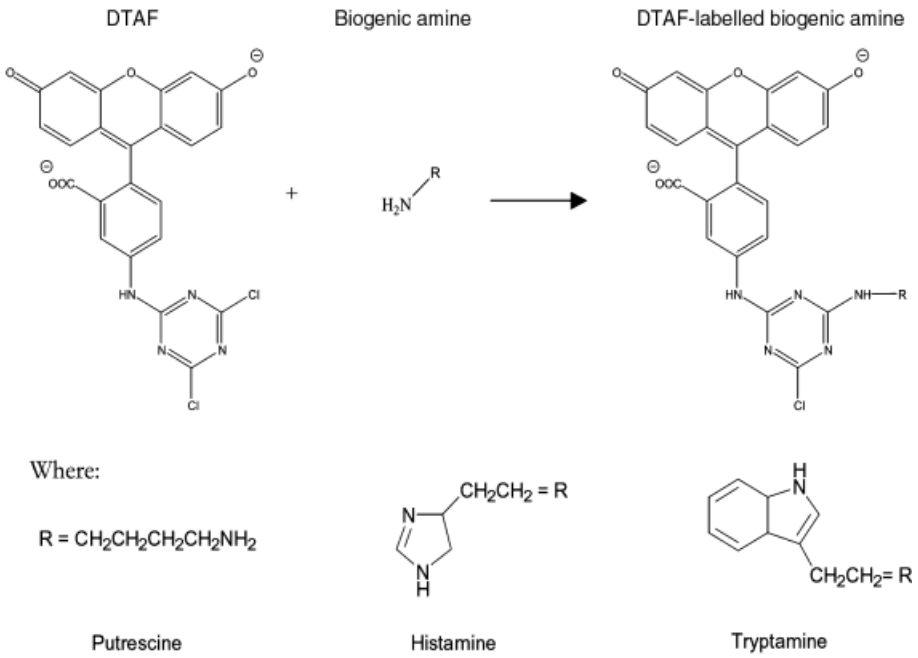

Figure 3. Scheme of the derivatization reaction between DTAF and biogenic amines.

In an attempt to further establish whether DTAF can act as a stable and quantifiable derivatizing agent on conjugation with biogenic amines, fluorescent lifetimes of the free and bound forms were measured. This allows assessment of changes in photophysical properties of the dye on binding. Time resolved fluorescence measurements were carried out using the TCSPC described previously. The obtained decay curves were analyzed using an iterative re-convolution procedure. For the present systems, the observed decay curves were seen to fit well to a single-exponential function (Eq. 3), with reduced chi-square (χ^2) values close to 1.

$$I(t) = A\exp\left(\frac{-t}{\tau}\right) \quad (3)$$

Here, τ is the fluorescence lifetime and A is the pre-exponential factor. Fig. 4 illustrates fluorescence decay profiles for free and bound DTAF with each of the biogenic amines accompanied by their respective residual plots. Statistical information resulting from decay curve analysis is presented in Table 2. The results indicate that the radiative decay properties of DTAF do not change significantly on binding and hence the label is suitable for quantification purposes. It should be noted that the fluorescence lifetime generated from the analysis of DTAF at an elevated concentration of 250 μM is significantly higher than in all other cases (4.55 ns). This information is included to demonstrate that DTAF shows no evidence of dimer formation at such concentrations (since the decay can be described by a single exponential decay law). The 20% increase in the observed fluorescence lifetime is simply due to fluorescence re-absorption effects, and is expected as such concentrations.

Table 2. Parameters resulting from a free sum-of-exponential analysis of fluorescence decay curves of DTAF and DTAF-biogenic amines

Analyte	τ_1 (ns)	Yield (%)	χ^2 (ns)	Durbin-Watson
DTAF-putrescine	3.8741	100	0.9413	1.5882
DTAF-histamine	3.8088	100	1.0991	1.5365
DTAF-tryptamine	3.8470	100	1.0892	1.3611
DTAF (25 μM)	3.8435	100	0.9802	1.5430
DTAF (250 μM)	4.551	100	0.8685	1.7190
Rhodamine 110 (standard)	4.1908	100	0.8463	1.8788

All data were obtained using J-Life© decay analysis software.

3.3 *In situ* derivatization of common biogenic amines with DTAF

There are numerous naturally occurring biogenic amines present in a variety of foodstuffs [3–10]. The following were selected to assess the performance of the derivatizing agent and the microdevice; putrescine (put), his-

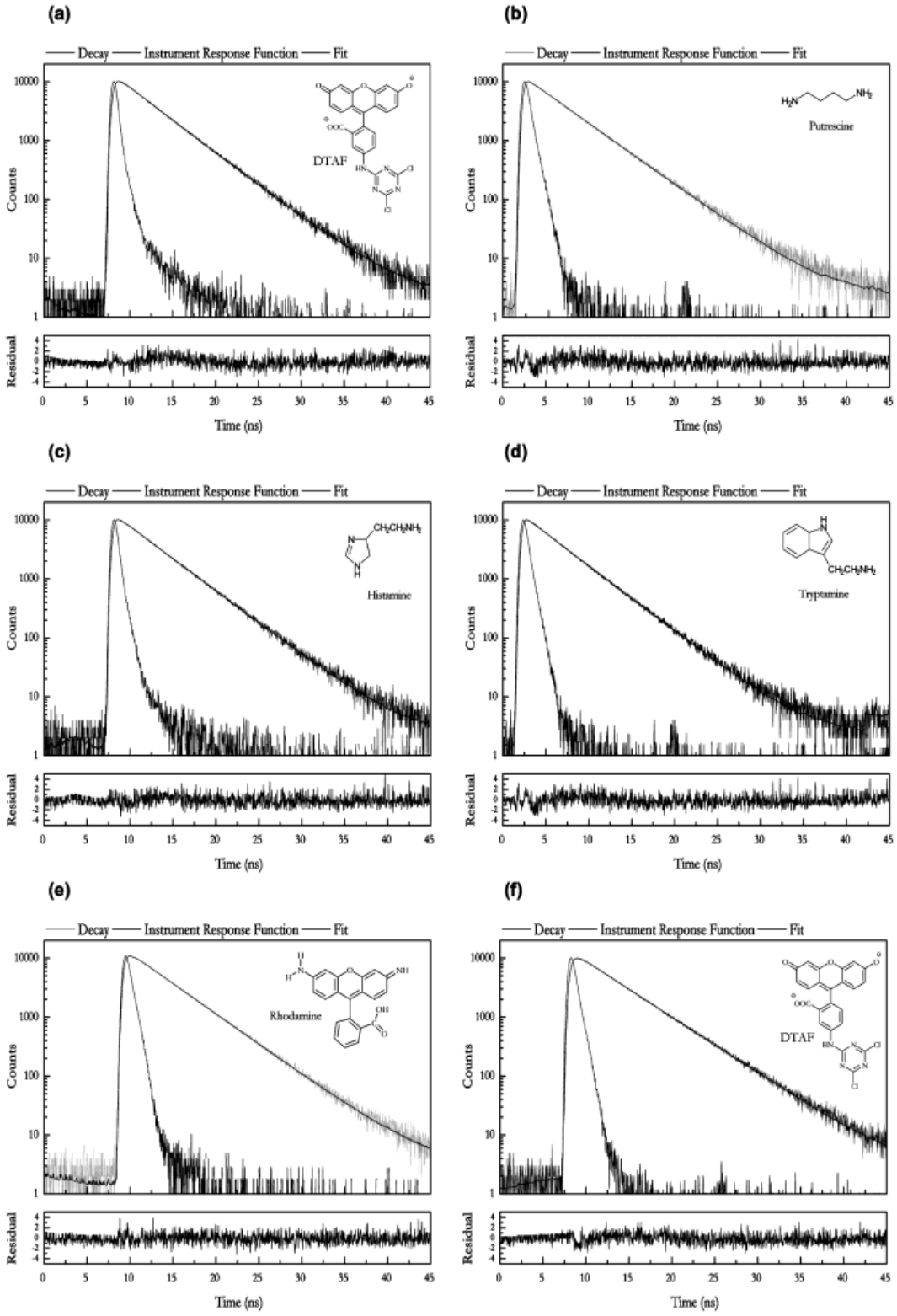

Figure 4. Fluorescent lifetime decays, instrument response function and fits resulting from two component global analyses of the DTAF-biogenic amines solutions. Amine concentration, 25 μM. (a) DTAF unbound (25 μM), (b) DTAF-put (10:1), (c) DTAF-his (10:1), (d) DTAF-trp (10:1), (e) standard (rhodamine 110, 25 μM), (f) concentrated DTAF (250 μM). All solutions were prepared in 80 mM borate buffer, pH 9.2.

tamine (his), and tryptamine (trp). Figure 5a illustrates a typical electrophoretic separation of these three biogenic amines (150 nM) after *in situ* labeling with DTAF (3 μM). The order of elution was confirmed by single component injections (data not shown) of each amine and identification by migration time. On labeling with DTAF, the resulting dye:amine complex is anionic. The pH of the separation buffer was adjusted to ~9.2, facilitating baseline separation between all the three amines. At this pH the fluorescence of the fluorescein moiety is also stabilized, due to the fact that the phenolic function is fully ionized [40]. The results illustrated in Fig. 5a demonstrate that the analysis of the three biogenic amines (including mixing, reaction and separation time) can be achieved in < 60 s. This represents a significant improvement when compared to previous reports. To ensure that the maximum derivatization yield was achieved during the mixing zone, the ratio of the number of dye molecules to analyte molecules was investigated. Figure 5b shows that increasing this ratio resulted in an improvement in the derivatization yield. However, further increases the DTAF: amine ratio beyond 20:1 did not significantly improve the yield of the labeled amine. This observed trend was also re-iterated for all the three biogenic amines studied. It is also worth noting that the observed electropherograms contain no apparent additional peaks from hydrolysis related side products.

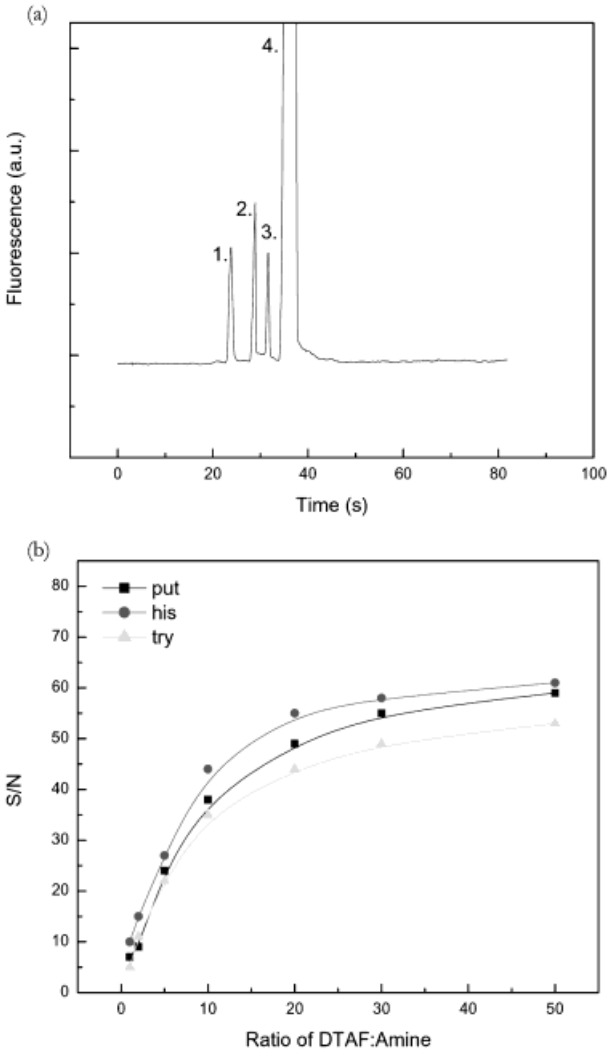

Figure 5. (a) Electropherogram recorded for CZE separation of DTAF-labeled biogenic amine standards. Running buffer, 80 mM borate adjusted to pH 9.2. The concentration of all analytes in the aqueous standard was 150 nM. DTAF concentration, 3 μM. A voltage of +3.0 kV was applied at the buffer inlet reservoir (12); the buffer outlet reservoir (13) was grounded. The detection window was positioned 30 mm downstream of the injection intersection. Peak assignment: 1, tryptamine; 2, histamine; 3, putrescine; 4, excess DTAF. (b) Influence of DTAF:biogenic amine ratio on derivatization yield. Concentrations of biogenic amines were constant at 50 nM. Other conditions were the same as in Fig. 5(a). Biogenic amine identification: (▲) tryptamine, (●) histamine (■) putrescine.

3.4 Reproducibilities, efficiencies, and detection limits

Table 3 provides a summary of the reproducibility data relating to the current microdevice. Here both the migration times and peaks areas for the same day analyses are adequate for all three amines. The interday deviations are slightly higher, and are most likely due to the experimental differences in solution makeup, and variations in EOF on a day-to-day basis. Efficiencies are quoted in terms of plate number and plate height. Improvements to these performance indicators could be realized by performing the separation in a MEKC mode (with the use of a micelle in the running buffer). However, optimization of micelle concentration would be necessary, adding to the complexity of the separation mode. In the current system, the entire analysis time is approximately 60 s and separation is achieved with good plate numbers.

The detection limits provided by the DTAF moiety provide strong support of its use in the analysis of biogenic amines. The results presented demonstrate detection limits of approximately 1 nM for the biogenic amines analyzed. This represents an improvement in excess of two orders of magnitude over the current literature values reported. For example, a limit of detection of around 1 μM has been reported for FITC-labeled biogenic amines by Li and co-workers [21], and more recently 0.1 μM using LIF for OPA-labeled biogenic amines by Hahn *et al*. [28]. In a previous paper we demonstrated that detection limits of ~3 μM could be obtained using indirect fluorescence detection [22]. However, this method of *in situ* labeling

Table 3. Reproducibility, detection limit and column efficiency data for the integrated *in situ* labeling CE microdevice

Analyte[a)]	RSD[b)] peak area intra-day (%)	RSD[b)] peak area intra-day (%)	RSD[b)] migration time intra-day (%)	RSD[b)] migration time inter-day (%)	LOD (S/N = 3)	N[c)]	H[c)] (μm)
Tryptamine	2.45	6.62	2.23	5.15	2.0 nM	6400	3.90
Histamine	1.96	6.38	1.64	3.13	1.0 nM	9200	2.72
Putrescine	2.03	9.15	2.13	6.45	2.5 nM	9400	2.66

a) All the test samples were prepared in ethanol before dissolving in 80 mM borate buffer, pH 9.2. The concentrations of, putrescine, histamine, and tryptamine for RSD measurement were 150 nM and the concentration of DTAF was 25 μM. The voltages and running buffer are as for Fig. 5a. The data were obtained with separation lengths of 30 mm.
b) The RSDs for intra-day and inter-day were calculated from five measurements on the same day and different days, respectively.
c) Plate numbers (*N*) and plate height (*H*) were evaluated with a sample containing 150 nM putrescine, histamine, and tryptamine.

has afforded significantly lower detection limits and improved selectivity, whilst maintaining the rapid speed of total analysis provided by the IFD method.

3.5 Analysis of biogenic amines in Thai fish sauce

To demonstrate the applicability and robustness of both the microdevice and the labeling technique in real sample analysis, determination of biogenic amines in Thai fish sauce was performed using the optimum conditions defined previously. It is worth emphasizing that the Thai fish sauce was prepared using the most basic sample preparation technique, *i.e.*, dilution, and was introduced and analyzed on-chip in its natural state. Fig. 6a shows the separation of Thai fish sauce after *in situ* labeling with DTAF. Peaks representing putrescine and histamine were identified in the complex mixture, and confirmed by sample spiking with a 1 μM standard addition. However, it is noticeable that the observed electropherogram contains interfering peaks within the complex mixture. This is due to the nonspecific nature of the derivatizing agent to react with any analyte containing amino functionality. It is therefore conceivable that any additional analytes present such as amino acids or proteins would undergo the same labeling process with DTAF. In an effort to improve the discriminating power of the labeling technique, the Thai fish sauce was passed through a strong cation exchange column (HiTrap™ SPFF; Amersham Biosciences, Buckinghamshire, UK) prior to its introduction into the microchip. The resulting electropherogram in Fig. 6b demonstrates a 'cleaner' separation with fewer interfering peaks, permitting the biogenic amines to be more easily identified.

4 Concluding remarks

In this paper we have demonstrated a novel design and method of performing integrated *in situ* labeling of biogenic amines followed by efficient separation in the same device in times < 60 s. In doing so, we have highlighted some of the difficulties that need to be addressed when attempting to transfer traditional labeling techniques to chip-based formats. As a result, we also present DTAF as real alternative to FITC [21] and OPA [28] as an *in situ* label for the rapid analysis of amines. This is primarily due to the favorable photophysical properties and rapid labeling chemistries of DTAF, and the ability to perform rapid distributive mixing within the microfluidic system [43]. It has been shown that DTAF has an affinity to react quickly and effectively with biogenic amines, extending the arsenal of methods available for analysing such 'problem' analytes that contain no natural fluorophore or chromophore. We have presented detection limits down to 1 nM representing in excess of 2-orders of magnitude over previously reported results [28]. Not only is new method more sensitive, but it also provides inherent discrimination of interfering analytes due to the specificity of the derivatizing agent. This has been demonstrated through the identification of biogenic amines in a sample of Thai fish sauce with minimal sample pretreatment.

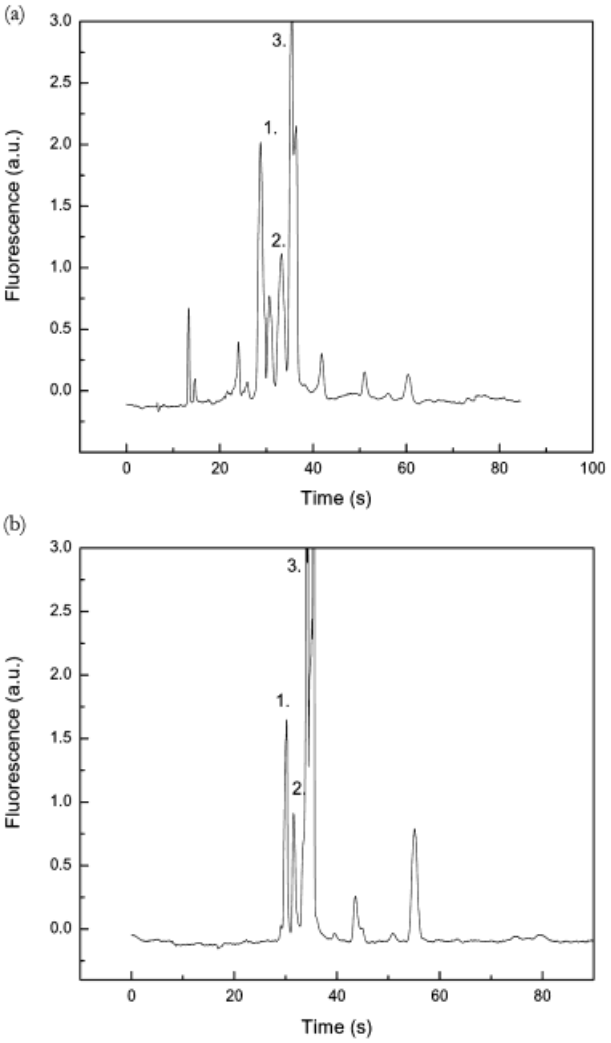

Figure 6. (a) CZE separation of DTAF-biogenic amines in a Thai fish sauce sample. Peak identification: 1, histamine; 2, putrescine; 3, excess DTAF. (b) CZE separation of DTAF-biogenic amines in a Thai fish sauce sample after passing through a strong cation exchange column. Peak identification: 1, histamine; 2, putrescine; 3, excess DTAF. All other conditions were the same as in Fig. 5a.

The benefits of performing integrated, *in situ* labeling on-chip not only incorporate reduction in cost and low reagent consumption, but also include vastly reduced analysis time, reduction in problematic hydrolysis products and enhanced detection limits. Finally it should be noted that conventional systems will also benefit from the development of new labeling chemistries. The DTAF moiety has proven to be excellent for the analysis of biogenic amines. Nevertheless, the affinity of the labeling moiety for any analyte containing the amino functionality means that analysis of species such as proteins and amino acids is also possible. Current work is focusing on such a diversity of analytes and applications, alongside the integration of more complex sample preparation techniques onto monolithic substrates.

The authors would like to acknowledge EPSRC UK and Unilever Ltd. for financial support and Dr. Omar Naji for fabrication of the electrophoresis power supply.

Received October 10, 2003

5 References

[1] Stratton, J. E., Hutkins, R. W., Taylor, S. L., *J. Food Protect.* 1991, *54*, 460–470.

[2] Eccelston, D., Crawford, T. B. B., Ashcroft, G. W., *Nature* 1963, *197*, 502–503.

[3] Fernadez-Garcia, E., Tomillo, J., Nunez, M., *Int. J. Food Microbiol.* 1999, *52*, 189–196.

[4] Nouadje, G., Nertz, M., Verdeguer, Ph., Couderc, F., *J. Chromatogr. A* 1995, *717*, 335–343.

[5] Arce, L., Rios, A., Valcarcel, M., *J. Chromatogr. A* 1998, *803*, 249–260.

[6] Busto, O., Guasch, J., Borrull, F., *J. Chromatogr. A* 1995, *718*, 309–317.

[7] Rodriguez, I., Lee, H. K., Li, S. Y. F., *Electrophoresis* 1999, *20*, 1862–1868.

[8] Rodriguez, I., Lee, H. K., Li, S. Y. F., *J. Chromatogr. A* 1996, *745*, 255–262.

[9] Oguri, S., Yoneya, Y., Mizunuma, M., Fujiki, Y., Otsuka, K., Terabe, S., *Anal. Chem.* 2002, *74*, 3463–3469.

[10] Kovacs, A., Simon-Sarkadi, L., Ganzler, K., *J. Chromatogr. A* 1999, *836*, 305–313.

[11] Handly, N., *Med. J.* 2001, *2*, 2–8.

[12] Roman, D., *Br. J. Psychiatr.* 1972, *121*, 619–620.

[13] You, J. M., Zhang, Y. K., *Chromatographia* 2002, *56*, 43–50.

[14] Shakila, R. J., Vasundhara, T. S., Kumudavally, K. V., *Food Chem.* 2001, *75*, 255–259.

[15] Romero, R., Sanchez-Vinas, M., Gazquez, D., Bagur, M. G., Cuadros-Rodriguez, L., *Chromatographia* 2001, *53*, 481–484.

[16] Rodier, D. R., Birks, J. W., *Chromatographia* 1994, *39*, 45–50.

[17] Molina, M., Silva, M., *Electrophoresis* 2002, *23*, 2333–2340.

[18] Male, K. B., Luong, J. H. T., *J. Chromatogr. A* 2001, *926*, 309–317.

[19] Chen, Z., Wu, J., Baker, G. B., Parent, M., Dovichi, N. J., *J. Chromatogr. A* 2001, *914*, 293–298.

[20] Arce, L., Rios, A., Valcarcel, M., *Chromatographia* 1997, *46*, 170–176.

[21] Rodriguez, I., Lee, H. K., Li, S. Y. F., *Electrophoresis* 1999, *20*, 118–126.

[22] Beard, N. P., deMello, A. J., *Electrophoresis* 2002, *23*, 1722–1730.

[23] Spikmans, V., Lane, S. J., Leavens, B., Manz, A., Smith, N. W., *Rapid Commun. Mass Spectrom.* 2002, *16*, 1377–1388.

[24] Gottschlich, N., Culbertson, C. T., McKnight, T. E., Jacobson, S. C., Ramsey, J. M., *J. Chromatogr. B* 2000, *745*, 243–249.

[25] Fluri, K., Fitzpatrick, G., Chiem, N., Harrison, D. J., *Anal. Chem.* 1996, *68*, 4285–4290.

[26] Harrison, D. J., Fluri, K., Chiem, N., Tang, T., Fan Z. H., *Sens. Actuators B* 1996, *33*, 105–109.

[27] Jacobson, S. C., Hergenroder, R., Moore, A. W. Jr., Ramsey, J. M., *Anal. Chem.* 1994, *66*, 4127–4132.

[28] Ro, K. W., Lim, K., Kim, H., Hahn, J. H., *Electrophoresis* 2002, *23*, 1129–1137.

[29] Lurie, I. S., Conver, T. S., Ford, V. L., *Anal. Chem.* 1998, *70*, 4563–4569.

[30] Lin, C. C., Lee, G. B., Chen. S. H., *Electrophoresis* 2002, *23*, 3550–3557.

[31] Huang, T. M., Pawliszyn, J., *Electrophoresis* 2002, *23*, 3504–3510.

[32] Chien, F. L., Bousse, L., *Electrophoresis* 2002, *23*, 1862–1869.

[33] Chen, S. H., Lin, Y. H., Wang, LY., Lin, C. C., Lee, G. B., *Anal. Chem.* 2002, *74*, 5146–5153.

[34] Kerby, M. B., Chien, R. L., *Electrophoresis* 2002, *23*, 3545–3549.

[35] Kerby, M. B., Spaid, M., Wu, S., Parce, J. W., Chien, R. L., *Anal. Chem.* 2002, *74*, 5175–5183.

[36] Kerby, M. B., Chien, R. L., *Electrophoresis* 2001, *22*, 3916–3923.

[37] Chien, R. L., Parce, J. W., *Fresenius' J. Anal. Chem.* 2001, *371*, 106–111.

[38] Deshpande, M., Greiner, K. B., West, J., Gilbert, J. R., Bousse, L., Minalla, A., *Proceedings of MicroTAS 2000*, Enschede, The Netherlands, 2000, pp. 339–342.

[39] Bousse, L., Minalla, A., West, J., *Proceedings of MicroTAS 2000*, Enschede, The Netherlands, 2000 pp. 415–418.

[40] Siegler, R., Sternson, L. A., Stobaugh, J. F., *J. Pharm. Biomed. Analysis* 1989, *7*, 45–55.

[41] Banks, P. R., Paquette, D. M., *Bioconjugate Chem.* 1995, *6*, 447–458.

[42] van Dalen, J. P. R., Haaijman, J. J., *J. Immunol. Methods* 1974, *5*, 103–106.

[43] Bessoth, F. G., deMello, A. J., Manz, A., *Anal. Commun.* 1999, *36*, 213–215.